

Development of an AUTODESK CFD Based 3D Model of a Hall-Héroult Cell Hooding System HF Capture Efficiency

Marc Dupuis¹, Michaël Pagé² and Frédéric Julien³

1. Consultant, GeniSim Inc, Jonquière, Canada

2. Owner associate, Simu-K inc, St-Nazaire-Du-Lac-St-Jean, Canada

3. Business Development Manager, Estampage JPL Ltd, Trois-Rivières, Canada

Corresponding author: marc.dupuis@genisim.com

Abstract

A full 3D model of a section of a Hall-Héroult anode cover and hooding system was developed using the code AUTODESK CFD. The model solves the thermo-electric behavior of the anode, the radiation between the solid surfaces in the model and the air flow inside and outside the cell hooding system. In addition of the heat dissipated by the anode panel, the model takes into account the production or evolution of hot CO, CO₂ and HF by the cell and the combustion of the CO at the surface of the crust as source of heat. The model directly solves for the concentration of HF in the gas, so the cell hooding HF capture efficiency is directly predicted by the model taking into account all the physics involved.

Keywords: Cell hooding efficiency, CFD, HF capture, HF emission

1. Introduction

The cell hooding design and the HF capture efficiency are important aspects of a cell design. This is true today but it will become even more important in the future as in addition to the aim of maintaining a very high HF capture efficiency, the desire to further reduce the environmental impact of the Hall-Héroult process will lead to cell designs dissipating less and less heat through the anode panel. This could be done by increasing the gas temperature under the hood and using the heat of the exhaust gas to produce electricity and even by capturing the cell CO₂ emission. In order to achieve those objectives, the exhaust gas suction rate will need to be significantly decreased in order to increase that average gas temperature under hood and increase the CO₂ concentration in that exhaust gas while maintaining a very high HF capture efficiency. This in turn translates into the need to design a very tight superstructure and hooding panels system and hence the need to design hooding panels that will resist higher gas temperature under the hood without mechanically weakening or deforming too much and limit the heat loss through them.

In order to be able to predict the cell hooding HF capture efficiency and hooding panels operating conditions under a wide range of cell operating conditions like cell amperage, anode cover thickness and especially hooding design and exhaust gas sucking rate, a full 3D model of a section of a Hall-Héroult anode panel and hooding system was developed using the code AUTODESK CFD.

2. AUTODESK CFD Full 3D Model of a Section of a Hall-Héroult Anode Panel and Hooding System

The full model will include both the 3D thermo-electric model of the anode, the 3D CFD model of the gas under the hood and outside in the potroom and the solid surface to solid surface radiation exchange model. As a first step, the 3D thermo-electric model of the anode was developed in order to reproduce using AUTODESK CFD the ANSYS based 3D thermo-electric model previously published [1].

2.1. AUTODESK CFD 3D Thermo-electric Model of the Anode

The model developed in this work is only a demonstration model so it is not reproducing any commercially available cell design. The anode geometry is the same geometry as the previously published ANSYS based demonstration 3D thermo-electric model, itself inspired from the VAW 300 cell design published in 1994 [2].

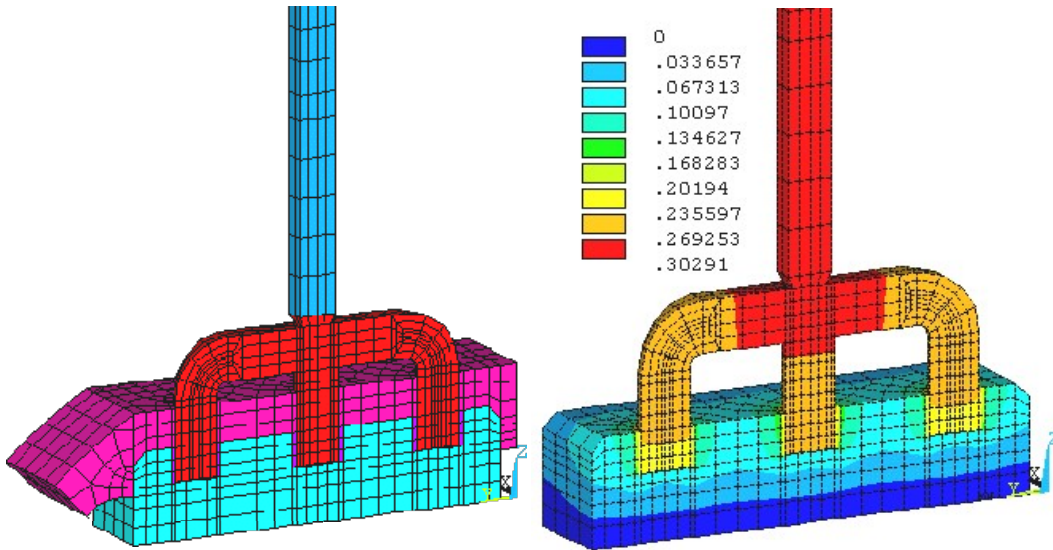


Figure 1. ANSYS based 3D thermo-electric demonstration model from [1]

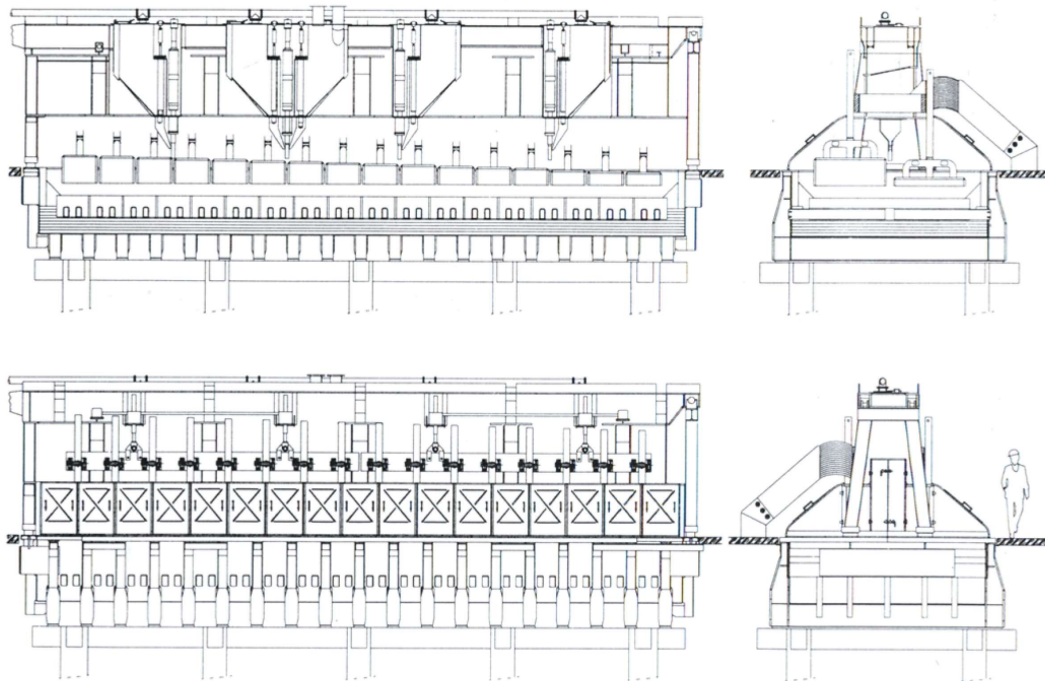


Figure 2. Sketch of the VAW 300 cell design from [2]

The VAW 300 cell was operating at 300 kA and was using 32 1.6 m x 0.8 m anodes. Each anode had 3 stubs in line. Using identical geometry and material properties and very similar combined convection and radiation boundary conditions but a much finer mesh, the AUTODESK CFD model results are very similar to the based ANSYS model.

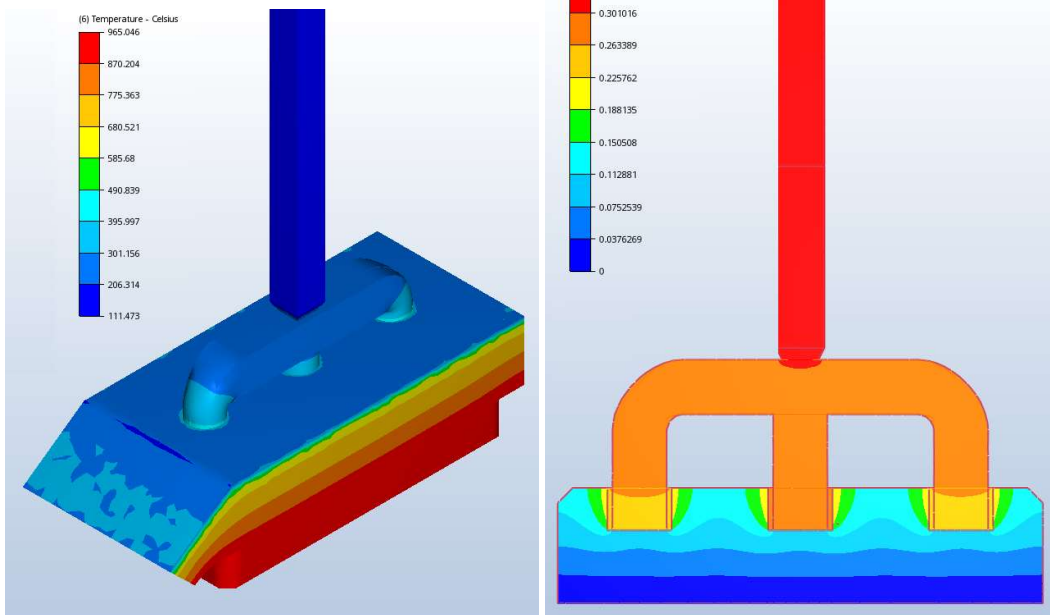


Figure 3. AUTODESK 3D based 3D thermo-electric equivalent model

2.2. AUTODESK CFD Full 3D Model of a Section of a Hall-Héroult Anode Panel and Hooding System

2.2.1. Model Geometry

The full AUTODESK CFD model is composed of 4 such anodes and the superstructure above them. The geometry of the superstructure is also generic and public domain. This time, it is inspired from a very similar model recently published [3]. The section of superstructure contained two quarter sections of feeders and half of an exhaust duct. The model also contains 5 hooding panels, the geometry of those hooding panels was provided by Estampage JPL. It is the only part of the model that represents a commercially available product (see Figure 5).

In order to predict the HF capture rate, it is important to not only model the gas flow under the hood but also to model part of the air flow in the potroom and even part of the air flow in the top section of the basement. For that reason, a section of the cement slab that separates the basement from the potroom is also part of the model. We can see a representation of that cement slab in Figure 2 sketch, the worker that is defining the scale is walking on it.

The model solid objects are presented in Figure 4, the stab section is floating on the right side, in front of the hooding panels and the section of the potshell wall and coverplate is represented in the model.

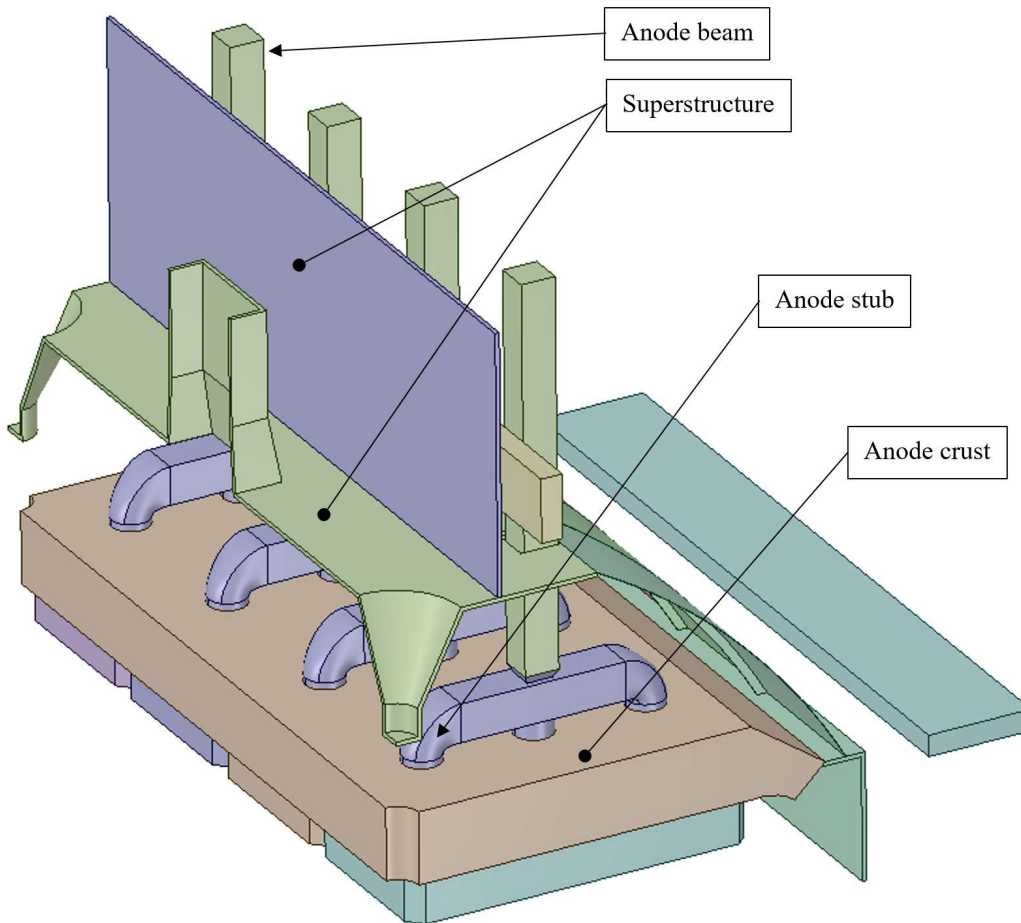


Figure 4a. Solid objects of the full AUTODESK 3D based model

Finally, a section of the anode beam is also in the model, that section being part of the thermo-electric submodel. The electric current is equally fed on both ends of that anode beam.

There are two types of solids in the models: 1) the thermo-electric solids: the anode beam and rods made of aluminium, the anode studs and yoke made of steel, the anode carbon blocks and the cast iron connections between the stubs and the anode carbon blocks; 2) the other solids: the anode crust, the aluminium hooding panels, the steel superstructure and the cement slab that all are thermal only solids.

2.2.2. Model Mesh

Fluid elements (in yellow) are added to the model inside the hood, in the top section of the basement and in the bottom section of the potroom, as seen in Figure 6. The fluid mesh in contact with solids is first meshed with very thin boundary layer elements that are required to accurately calculate the heat exchange by convection between those solids and the gas. Figure 7 is presenting an example of that boundary layer mesh. The mesh used in this study is made of about 7,000,000 fluid elements and about 2,600,000 solid elements.

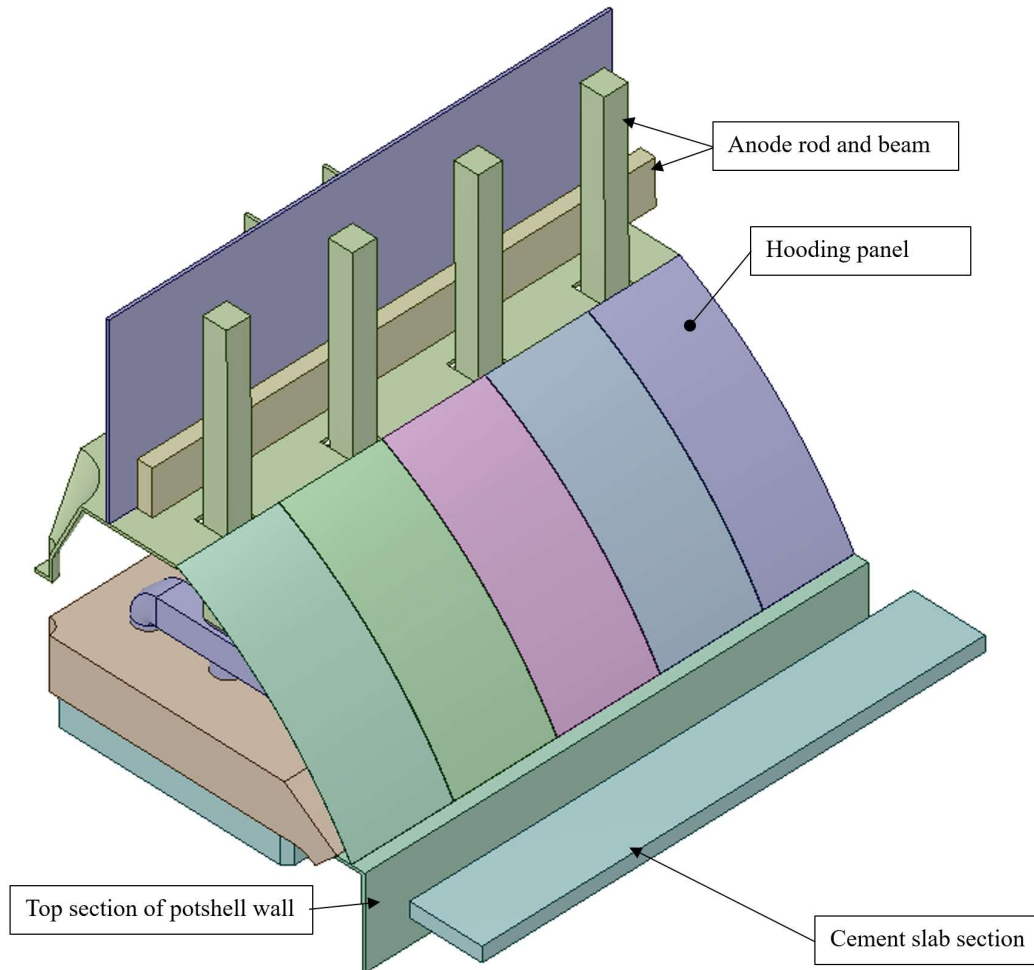


Figure 4b. Solid objects of the full AUTODESK 3D based model

2.2.3. Degree of Freedom Solved in the Model

The model was solved for the temperature in the full domain. In addition to the conduction in the solid elements and the convection and conduction in the fluid elements, there is a surface to surface radiation model to calculate the heat exchanged by radiation. This is important both to well represent the anode top surface heat losses and to well predict the hooding panels temperature and heat losses to the potroom by convection and radiation.

The voltage is solved in the thermo-electric solid elements. The Joule heating is then added to the temperature equation. Because of the accurate calculation of the heat transfer by convection and radiation on the anode top surfaces and the accurate calculation of the ambient temperature on top of the anode panel, the anode panel heat losses are calculated more accurately than when using a standard thermo-electrical anode model.

In AUTODESK CFD documentation, it is recommended to solve this mixed convection CFD flow problem using the low Mach number assumption [4]. For postprocessing purpose only, the static head removed from the momentum equations is added back. The turbulence is represented using the $k-\omega$ SST turbulence model [4].

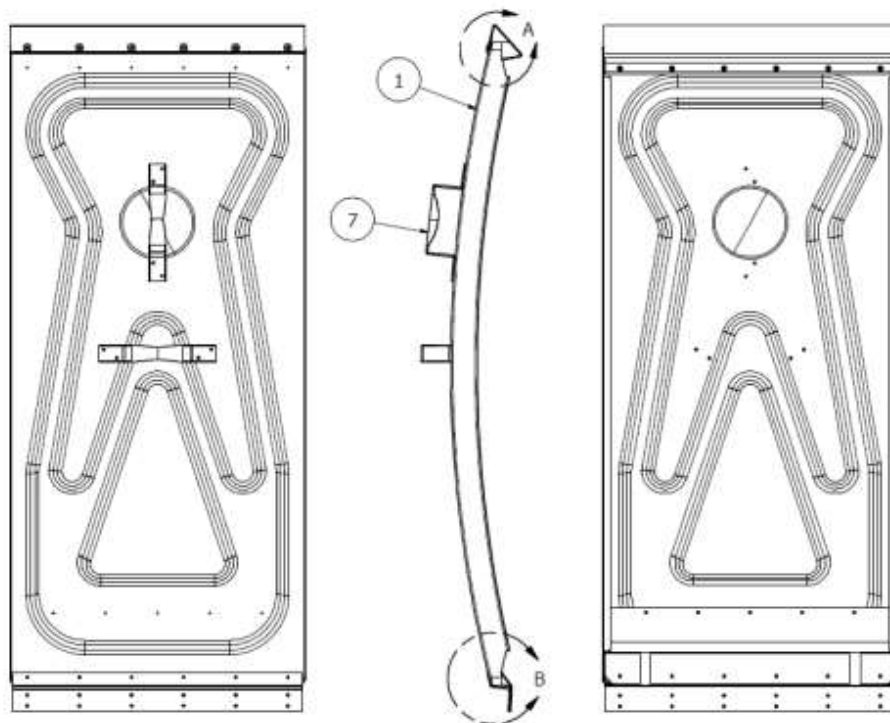


Figure 5. Geometry of the hood panel represented in the model

The gas under the hood is a mix of air, CO₂ and HF but it is treated as pure air as far as the gas properties are concerned. The cell also produces CO that is assumed to burn in CO₂ at the crust surface. The heat of combustion of that CO is added as an extra source term in the fluid elements in the crust holes at the surface.

The concentration of the HF in the gas is calculated using a passive scalar equation that is solved in extra. The HF capture efficiency is also calculated at the very end based on the HF concentration in the exhaust gas and the exhaust gas rate. It could also be independently calculated based on the HF concentration of the gas escaping from the hood and the escape gas rate. In the results presented here, no HF escaped in the potroom.

2.2.4. Boundary Conditions in the Model

There are many types of boundary conditions in that model. The first set is for the electrical voltage equation. The current is assumed to enter equally from both ends of the anode beam. The total current fed to the model is $4 / 32 * 300 = 37.5$ kA. So the anode current density is only $37500 / (160 \times 80 \times 4) = 0.73$ A/cm² which is the current density reported in [2]. The 0 volt reference potential is applied on the bottom face of the anodes.

There are heat flux boundary conditions on the solid faces not in contact with the fluids elements. On each of those solid surfaces a combination of heat transfer coefficient and ambient temperature is applied, per example 2000 W/m² °C and the bath temperature for the immersed part of the anode carbon blocks. The only exception is the forced temperature of the potshell coverplate (200 °C) and top section of the potshell side wall (300 °C). That section of potshell side wall in the basement is there only to trigger the natural convection air flow in the basement.

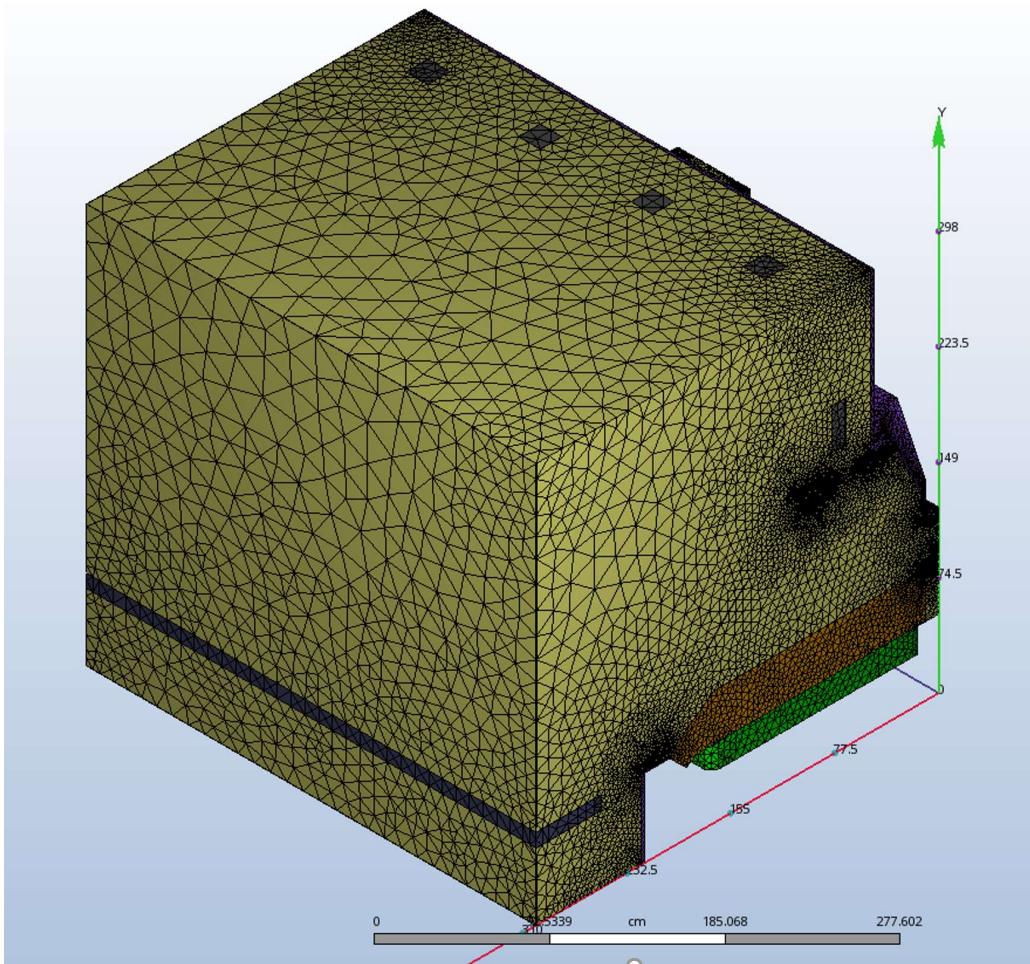


Figure 6. Mesh of the full AUTODESK 3D based model

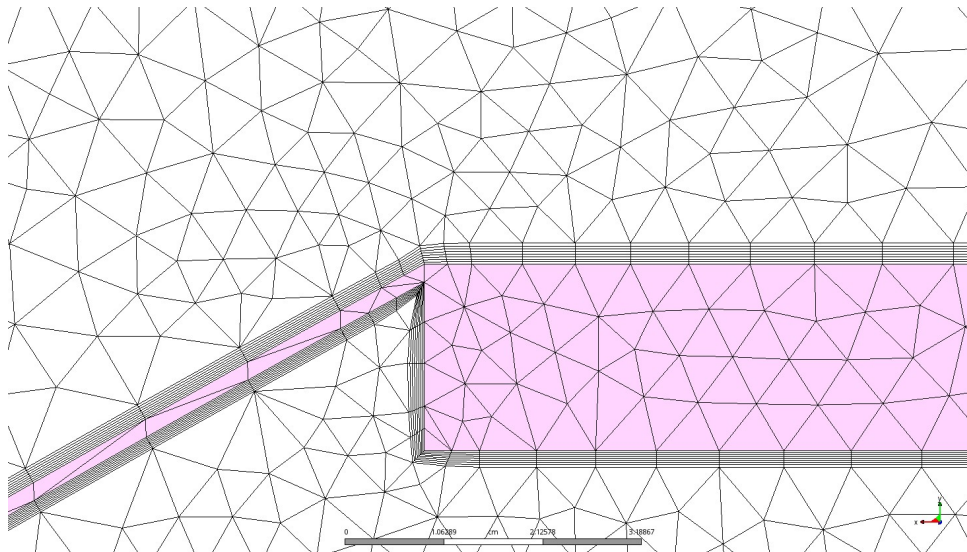


Figure 7. Zoom on the boundary layer mesh on the surface of the solid parts

For the CFD equations, the reference 0 pressure is fixed at the top surface of the model in the potroom. A very small uniform air inflow is imposed in the bottom face of the model in the basement. The natural convection air flow that developed in the basement is not imposed in any way so the air flow that enters the potroom from the basement is part of the model solution. The exhaust gas rate at the end of the exhaust duct is also imposed. In the study presented here, it was set to 0.3 Nm³/sec which represents 2.4 Nm³/sec for the full 300 kA cell.

Most of the exhaust gas is infiltrated air from the potroom. The remaining is the gas produced by the cell. Assuming 95% current efficiency, the equations presented in Peter Entner website [5] have been used to calculate the CO and CO₂ cell production. It turned out to be 110.835 kg CO₂/hr and 7.839 kg CO/hr. Once the CO is burned into CO₂ this gives 123.15 kg CO₂/hr that corresponds to a gas flow rate of 62.72 Nm³ CO₂/hr for the cell or 7.84 Nm³ CO₂/hr for the model equally split into the two quarter feeder crust holes. The burning of the CO is producing 22 kW for the full cell corresponding to 2.75 kW again equally split between the two quarter feeder crust holes.

For the HF production, assuming an evolution of 26.5 kg F/t Al, the cell is producing 2.535 kg F/hr or 2.67 kg HF/hr. That HF is not all emitted in its gaseous form but for the present study, it was assumed that all the HF evolved by the cell is in its gaseous form. This then corresponds to a production of 3.2 Nm³ HF/hr for the cell.

That 3.2 Nm³ HF/hr is added to the 62.72 Nm³ CO₂/hr and converted into air as far as the properties of the gas produced are concerned. So, the cell is assumed to produce 65.92 Nm³/hr of gas at the operating temperature corresponding to an “air” inflow of 4.12 Nm³/hr in the bottom of the two quarter feeder crust holes. That hot air will flow through the crust feeder holes and will receive the energy from the CO combustion when reaching the surface. In real cells, that CO combustion produces a visible flame that radiates heat, but that extra radiation is neglected in the current study as the radiation model available in AUTODESK CFD is only a solid to solid radiation model.

The concentration of HF is computed in the model using a passive scalar. The only source of that scalar is the two quarter feeding holes. The concentration of HF in those two inlets is calculated to be 2.67/ 65.92 = 0.0405 kg HF/Nm³. Assuming 100% HF capture efficiency, based on the dilution ratio, the average HF concentration in the exhaust gas should be reduced to:

$$65.93 / (2.4 \times 3600) \times 0.0405 = 0.000309 \text{ kg HF/Nm}^3 \quad (1)$$

2.2.5. Model Solution

The model is solved first in steady state mode using the ADV 5 (Modified Petrov-Galerkin) convergence scheme available in AUTODESK CFD [4]. In the current study, 300 iterations have been used to converge the steady state conditions. Computing that solution required 18h20 CPU using 6 Intel Xeon E2630 v2 processors operating at 2.6GHz on a computer having 64 GB of RAM.

After those 300 iterations, the selected convergence criteria were satisfied. Figure 8 presents the obtained voltage drop which is again very similar to the one obtained with the ANSYS based thermo-electric model. Figure 9 presents the obtained anodes temperature showing in particular the obtained surface temperature for the crust, stubs and yoke. The temperature was obtained considering the non-linear influence of the temperature of the hooding panels and the gas temperature and flow conditions under the hood. Figure 10 presents the predicted temperature of all the solid objects in the model.

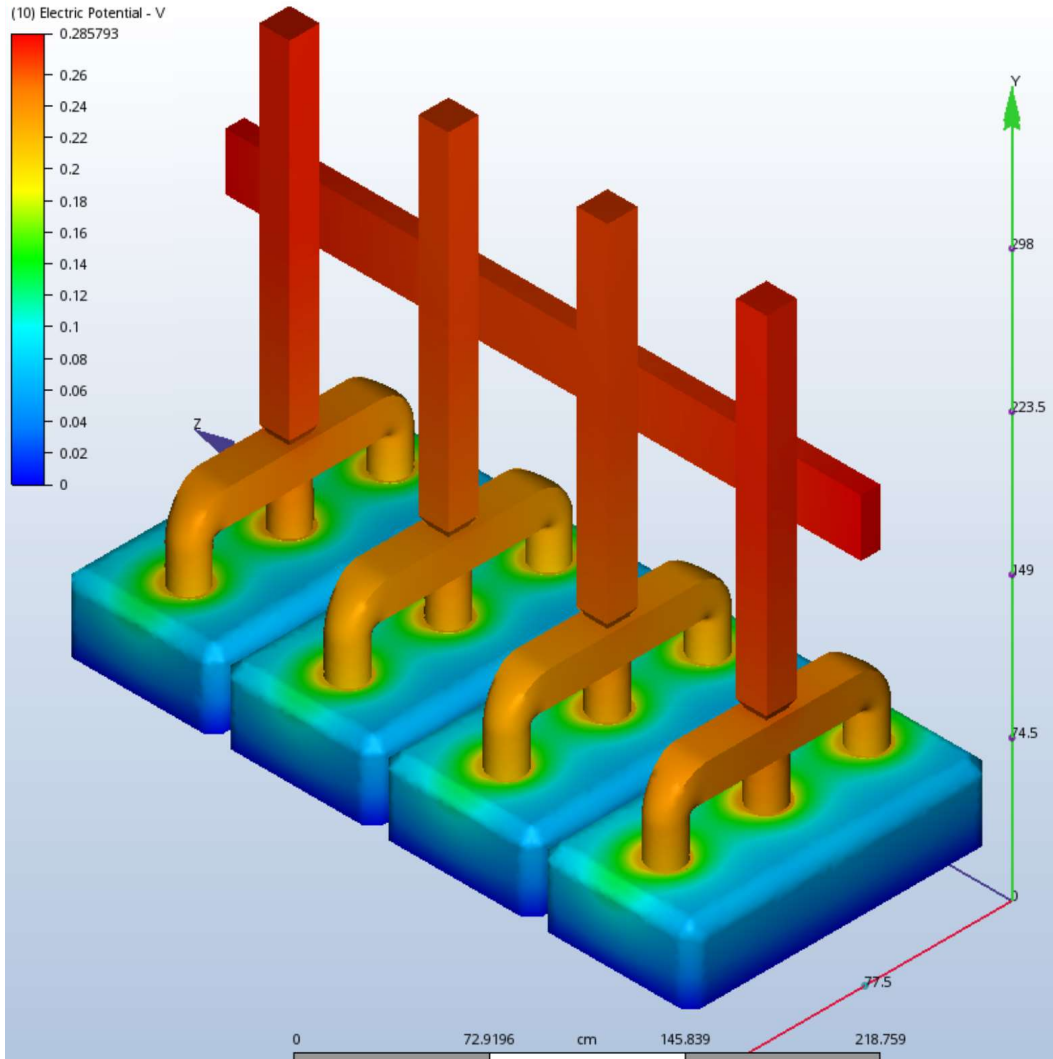


Figure 8. Obtained anode voltage drop

The resulting thermo-electric steady-state solution of the anodes and hooding panels is quite satisfactory. For the CFD solution, we can split it in two regions, the air flow in the potroom and the gas flow under the hood. Figure 11 is presenting the air flow solution, the potroom “2D” natural convection flow along the hooding panels and the superstructure is very well established. Figure 12 is presenting the corresponding air temperature solution also showing the corresponding “2D” natural convection plume in the potroom and the big temperature difference between the gas under the hood and the air in the potroom. It is also showing the “flame” location above the feeder crust hole. Finally, Figure 13 is presenting the corresponding air total pressure solution, dominated by the hydrostatic pressure variation. The proper solution of the pressure is important according to Dervedde [6] as it is the difference in the hydrostatic pressure gradient between the hot gas inside the hood and the colder potroom air that leads to HF leaks in the top region of the hood if the hoods openings are too big or the hood gas exhaust rate is too small to generate enough of a global pressure drop under the hood. In that circumstance, the pressure in the top region inside the hood becomes bigger that the potroom pressure at the same level and some hot gas with some HF contains is able to escape into the potroom. But this turned out not to be the case in the present study.

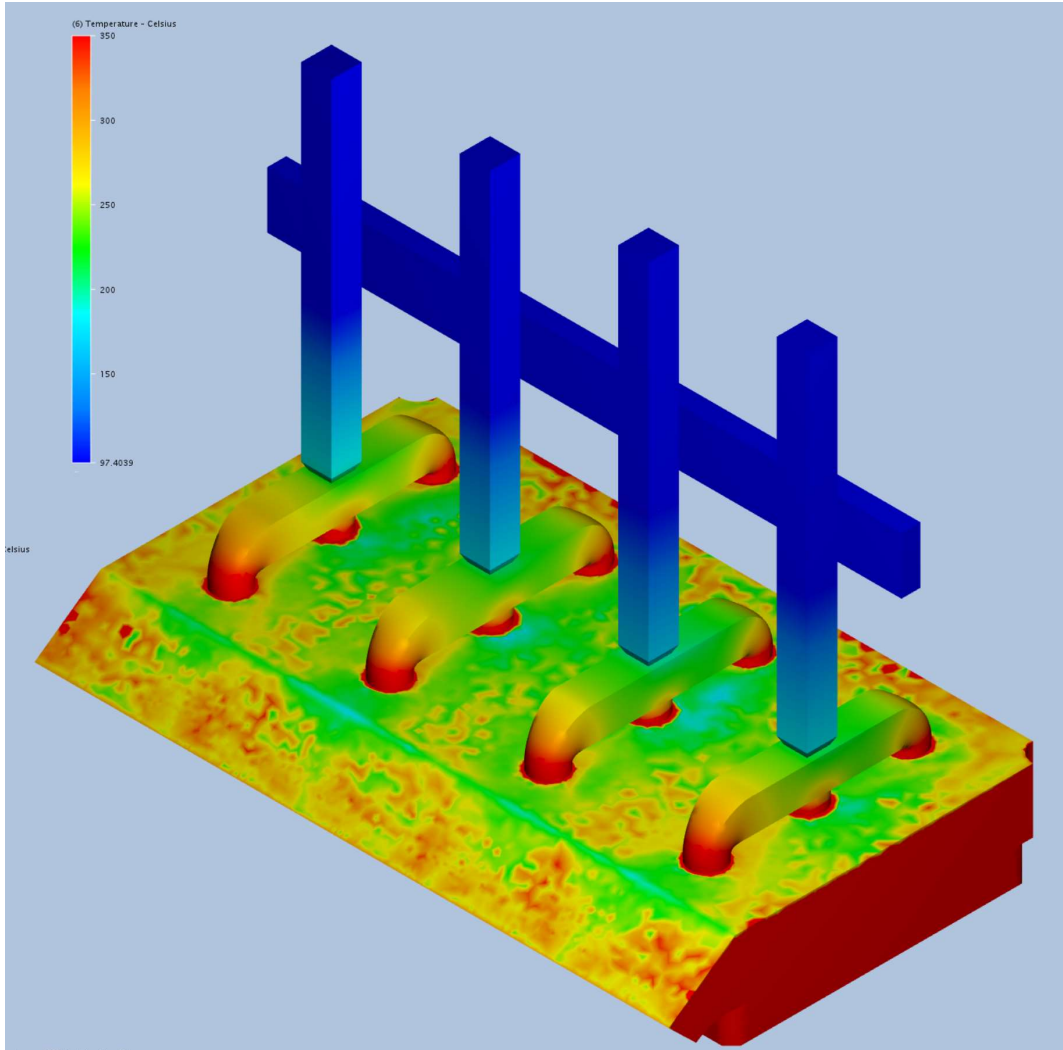


Figure 9. Obtained anode panel surface temperature

Despite the fact that no HF was escaping the hood, the calculated HF capture rate was far from 100% in the obtained “steady state” solution as expected. The converged steady state solution is also showing obvious signs of transient behavior despite the usage of a turbulence model. It was speculated that it is because the natural convection flow is in the transition regime in several regions of the flow domain. Figure 14 is showing the flow velocity solution in a vertical plane passing through the hooding panels. It highlights some secondary features of the flow like the air inlet in the small slots between panels. Those secondary flow features are clearly showing signs of transient behavior.

For that reason, it was decided to continue computing the flow evolution using the transient mode starting from that “steady state” initial condition. The flow evolution was computed for a period of 150 seconds using a 0.1 second time step with 3 equilibrium iterations per time step. Computing that transient evolution took 103h33 of additional CPU time.

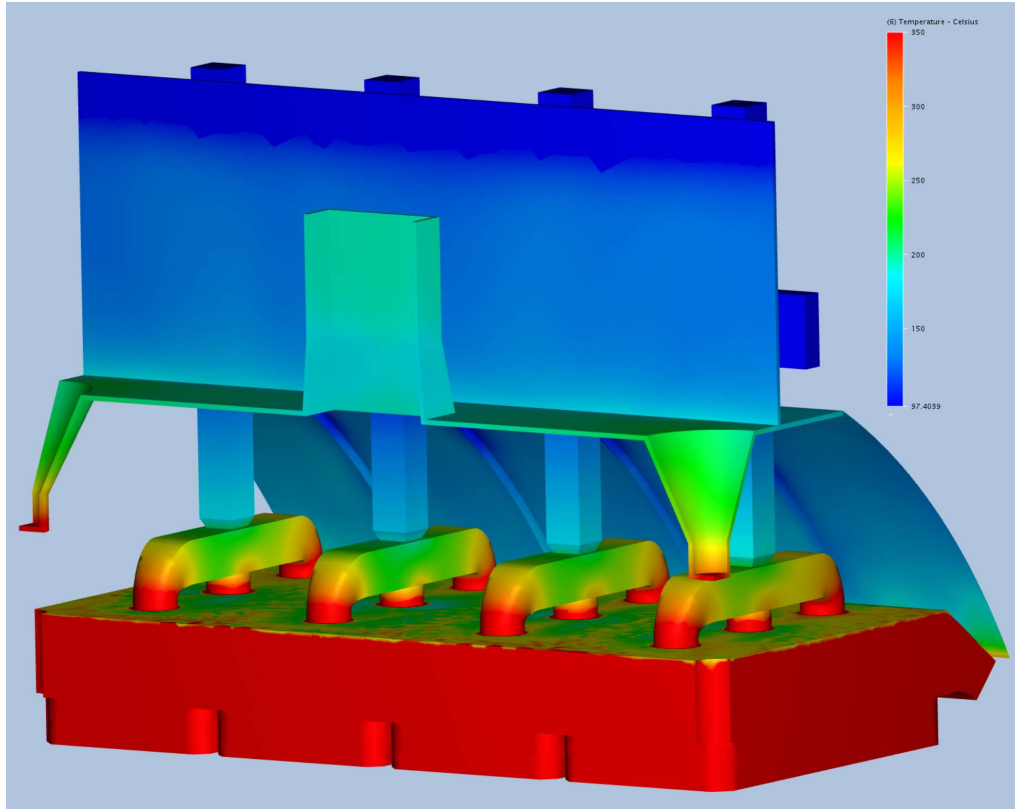


Figure 10. Obtained surface temperature of all solids in the model

Figure 15 presents the evolution of the instantaneous HF capture efficiency rate based on the previously computed expected $0.000309 \text{ kg HF/Nm}^3$ concentration assuming 100% capture based on the dilution rate. The instantaneous values randomly vary plus or minus 30% but the average value is 100 % plus or minus 1% for that full range of 150 seconds. Figure 16 is showing the instantaneous HF concentration at time 150 seconds of transient evolution showing clear signs of transient behavior. The selected $0.0005 \text{ kg HF/Nm}^3$ isosurface concentration represents 162% of the HF homogenous dilution concentration, all of the gas in the upper region of the hood is above that concentration and part of the exhaust gas leaves the hood above that concentration.

3. Conclusions

The aim of the current work was to demonstrate that it is possible to develop a model that reproduces well the complex physics occurring under the hood of a reduction cell. This includes the cell CO_2 , CO and HF gas production, the CO burning, the radiation heat transfer between solid surfaces and finally the gas circulation that dictates the convection heat transfer between the solid surfaces and the gas.

Part of the model solution is the calculation of the hooding panel temperature and heat loss to the potroom but the more important model prediction is the HF capture rate as function of the superstructure and hooding panels design and the gas exhaust rate. In the present study, the capture rate was 100% since no HF was escaping in the potroom. It turned out to be very difficult and expensive to calculate that HF capture rate efficiency based on the concentration of HF in the exhaust gas and the dilution rate as this concentration was not uniform in space nor constant in time.

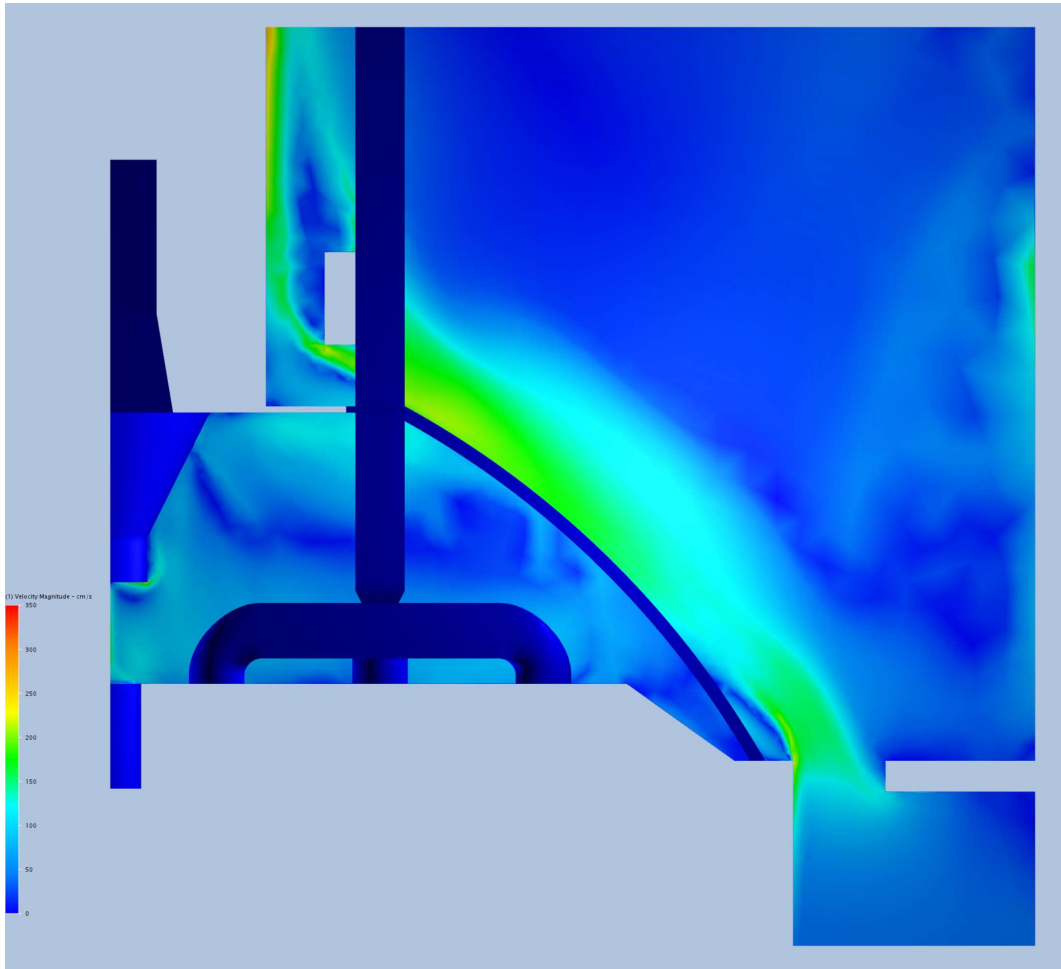


Figure 11. Obtained air flow velocity magnitude

4. Follow-up work

The present work is only the first step toward the development of a tool to design better hooding panels and better leak limiter around collector bars. This would allow a decrease in the gas exhaust rate while keeping the HF capture rate very close to 100%.

The next step will be to reproduce the current model Dervedde work [6] which consists of establishing the minimum gas exhaust rate for a given set of cell operating conditions, hooding panels and superstructure design. In order to do that, three new cases will need to be simulated using three reduced gas exhaust rate inferiors to the minimum gas exhaust rate to get some HF linkage into the potroom. The fit of the obtained HF capture rate as function of the gas exhaust rate using equation 20 in [6] will directly give a prediction of that minimum gas exhaust rate.

Once the minimum gas exhaust rate is established for the current hooding panels and superstructure design, a change of design affecting the size of the hood openings could be introduced in the model and the corresponding revised minimum gas exhaust rate established.

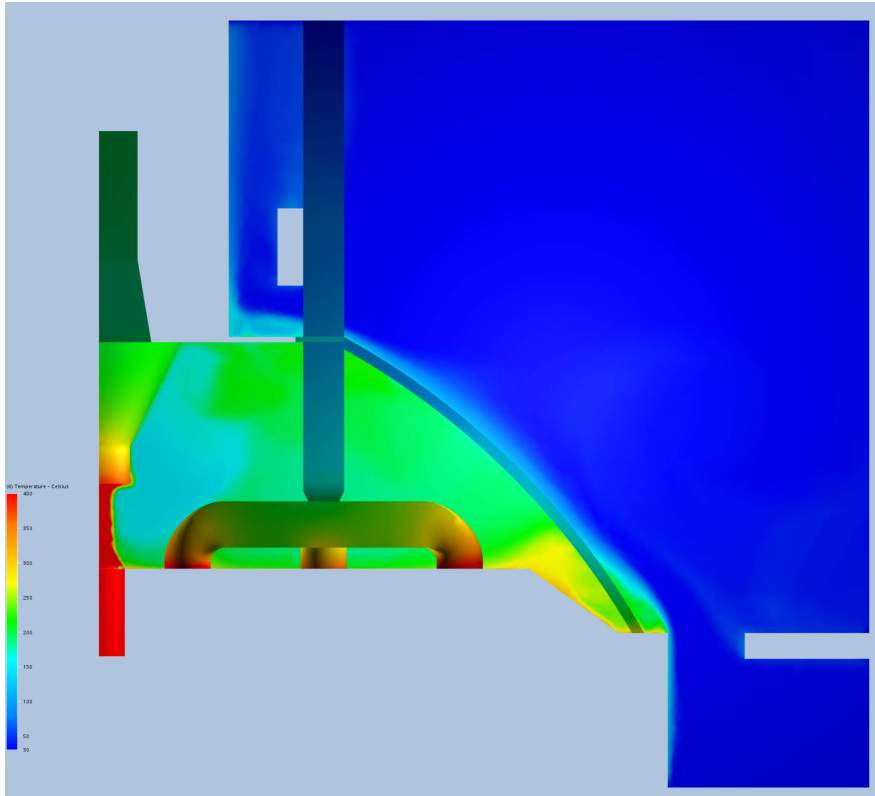


Figure 12. Obtained air temperature

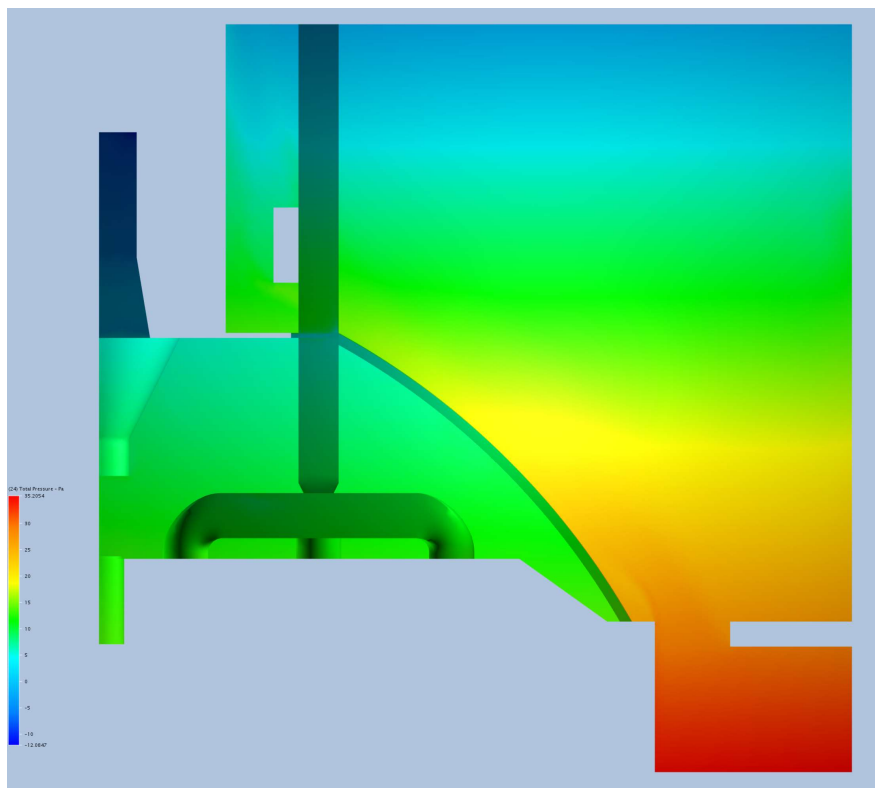


Figure 13. Obtained total air pressure

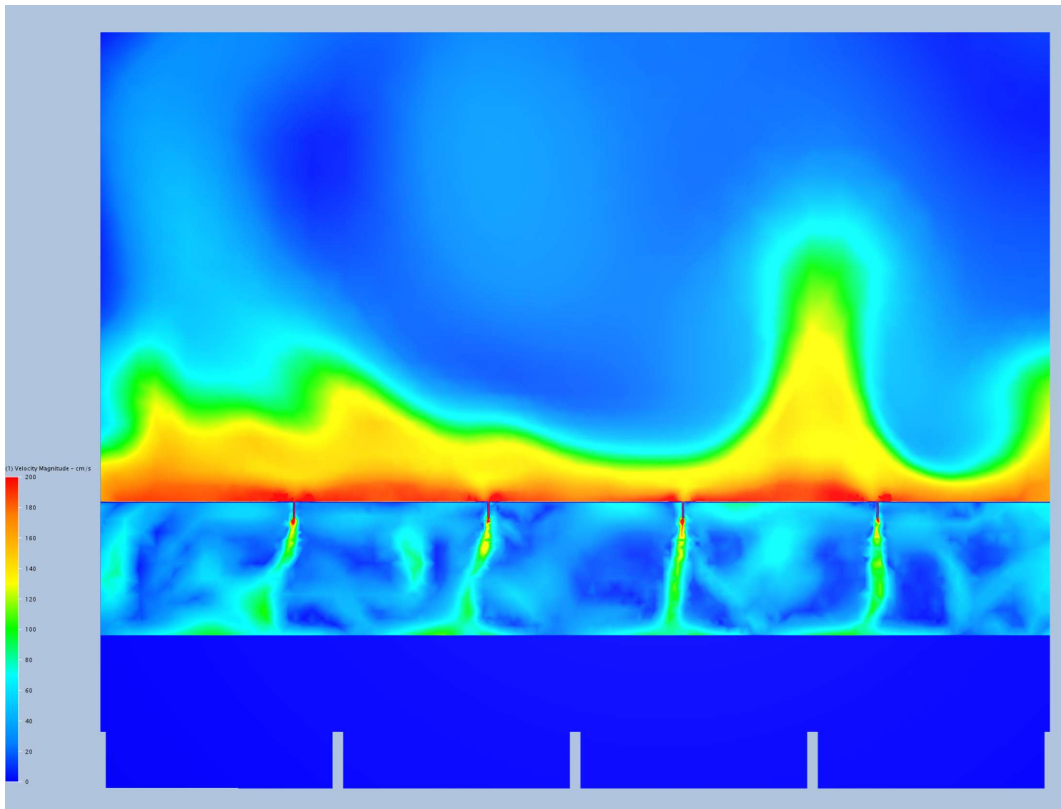


Figure 14. Obtained air flow velocity magnitude (vertical plane through panels)

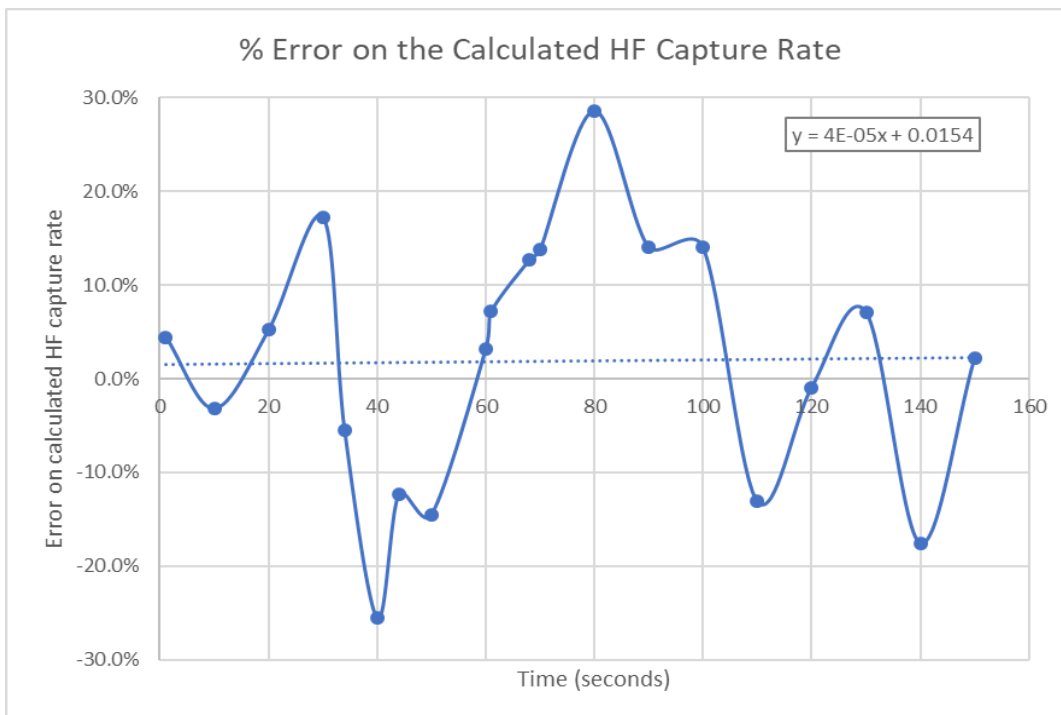


Figure 15. Deviation of the calculated HF capture rate from 100%

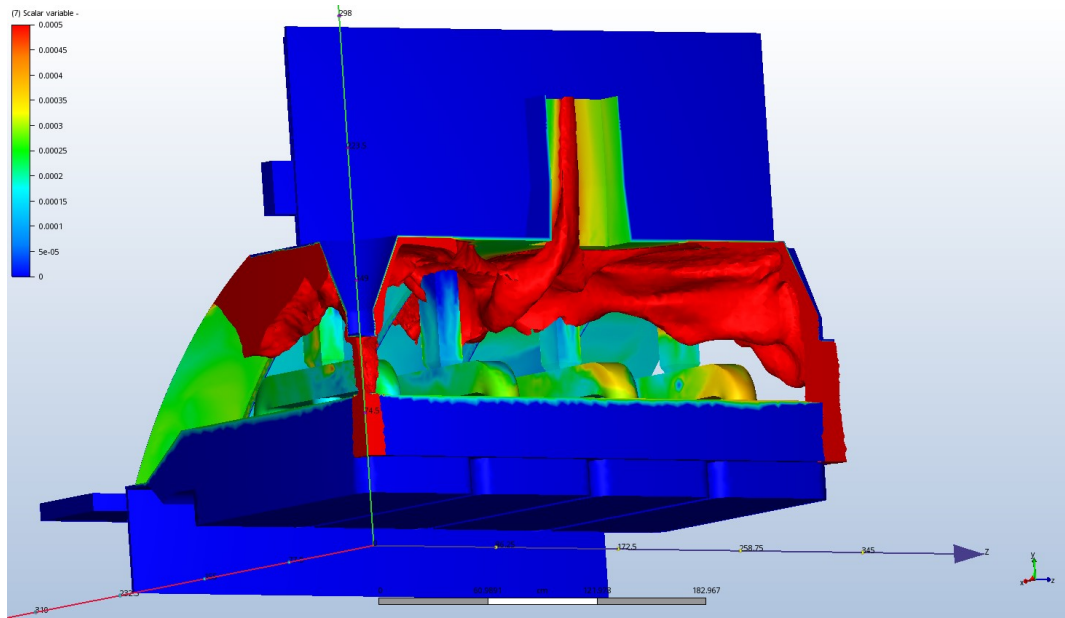


Figure 16. Isosurface of the HF concentration at 0.0005 kg HF/Nm³

5. References

1. Marc Dupuis, Computation of aluminum reduction cell energy balance using ANSYS[®] finite element models, *TMS Light Metals* 1998, 409-417.
2. Vasili A. Kryukovski, Gennady A. Sirasutdinov, Juergen Klein, and Gerald Pechal-Heiling, International cooperation and high-performance reduction in Siberia, *JOM*, Vol 46, No. 2, (1994), 23–25.
3. Ruijie Zhao, Louis Gosselin, Mario Fafard, Jayson Tessier and Donald P. Ziegler, Efficiency of pot tightness in reduced pot draft conditions based on multi-length scale CFD simulations, *International Journal of Thermal Sciences*, Vol 112, (2017), 395-407.
4. AUTODESK CFD 2017 Help Documentation, <https://knowledge.autodesk.com/support/cfd/downloads>
5. Peter Entner website, <http://www.peter-entner.com/E/Theory/MassB/MassB-1.aspx#PrincipalEquation>
6. Edgar Darnedde, Gas collection efficiency on prebake reduction cells, *American Industrial Hygiene Association Journal*, Vol 51, No. 1, (1990), 44-49.